



# DYNAMIC RESPONSE AND MOLECULAR SIMULATIONS OF NANO-COMPOSITES

Raju P. Mantena, Ahmed H. Al-Ostaz, Alexander H.D. Cheng,  
Composite Structures and Nano-Engineering Research,  
The University of Mississippi, University, MS 38677, USA

**Keywords:** *Dynamic modulus, damping, impact, MWCNT, molecular simulations*

## Abstract

*The dynamic modulus, damping, low-velocity impact, high-strain (Hopkinson bar) response and acoustic absorption coefficients of nanoparticle enhanced composites and fly ash based fire-resistant structural foams have been characterized. Molecular Dynamic (MD) simulations were used for obtaining the elastic constants for different matrices reinforced with single and multi-wall carbon nanotubes. Experimental results on the dynamic and impact response of nylon 6,6 thermoplastic with different weight-percents of multi-wall carbon nanotubes (MWCNT) and molecular simulations are presented in this paper.*

*An increase in dynamic modulus and marginal drop in damping was observed with the addition of multi-wall carbon nanotubes to pristine nylon 6,6. Low-velocity impact strength and energy absorption of un-notched and notched Charpy samples with MWCNTs was observed to be lower than nylon 6,6. However, the high-strain rate (~950/sec) response showed about a 10-20% increase in strength and energy absorption.*

## 1 Introduction

Fiber-reinforced polymer (FRP) composites are increasingly being used in naval platforms for improving the stealth and reducing topside weight, corrosion mitigation, fatigue, maintenance and operational costs. FRP composites are presently being used in US Navy Ships such as the Osprey class mine hunter, and for topside structures on large warships such as the Advanced Enclosed Mast System (AEMS). The navy also has plans to integrate more composites into the new generation CV(X) and DD(X) ship class designs. Structures in these applications are often subjected to high strain rates due to impact by hard objects, mine blasts, projectile penetration and collisions.

The Composite Structures and Nano Engineering Research Group at University of Mississippi is conducting research on dynamic and acoustic response, freeze-thaw effects, and molecular dynamic simulations of nanoparticle-enhanced composites and fly-ash based fire-resistant structural foams that are being developed for the future generation naval structures, or retrofitting of existing ones. Preliminary results from molecular simulations and experimental data on the dynamic and impact response of nylon 6,6 thermoplastic with different weight-percents of multi-wall carbon nanotubes (MWCNT) are presented in this paper.

## 2 Nanoparticle Enhanced Composite Plates

For this research, several 305 mm x 305 mm x 9.5 mm (12" x 12" x 0.375") thick nylon 6,6 thermoplastic plates reinforced with 1.25, 2.5, 5 and 10 weight percent multi-wall carbon nano tubes (MWCNT, supplied by Hyperion Catalysis) were prepared by Ensinger Inc. using a proprietary pressure extrusion process. A higher 20% weight loading of MWCNT resulted in plate fracture after extruding.

Attempts were also made to manufacture vinyl ester (VE) resins containing multi-wall carbon nanotubes at the Michigan State University Composite Materials and Structures Center, our collaborator on this project. Two loading levels were investigated, namely, 1.25 and 2.50 weight percent MWCNT in Derakane 411-350 vinyl ester resin. Each blend exhibited very high viscosity and tackiness, presenting significant processing challenges to uniformly distribute the curative package and remove entrapped air during consolidation. Small plates of 89 mm x 152 mm (3.5" x 6") were fabricated; however, these contained large voids and non-uniform properties across the parts. The high viscosity of the MWCNT-vinyl ester resin restricts removal of entrapped air, and plaques with acceptable quality were not produced. Scale-up to produce the 12 x 12 x 0.375 inch thick nano

composite plates that are needed for these investigations are expected to present even more difficulties to overcome. Manufacture of vinyl ester plates reinforced with low-cost fire resistant 1.25 and 2.5 weight percent nano clay and graphite platelets is currently in progress at Michigan State University.

### 3 Dynamic Modulus and Loss Factor

A non-destructive vibration response technique has been used to measure the dynamic flexural, extensional modulus and damping of the nanoparticle enhanced composites. For the flexural experiments, 254 mm x 25.4 mm (10" x 1") rectangular samples were cut from the plates for dynamic flexural modulus and damping measurements. The sample was clamped at one end in a vise and an accelerometer was placed at the free end. The specimen was excited by an impact hammer with a load cell inside. The hammer and accelerometer were connected to a spectrum analyzer via an amplifier. Note that the resonant frequencies obtained by this setup are of flexural mode. The spectrum analyzer is hooked to a computer with an in-house developed software ICARUS which calculates the dynamic modulus and loss factor (a measure of damping) based on the specimen dimensions, density and curve fitting the resonant peaks obtained from the spectrum analyzer [1]. Loss factor is calculated based on the 3 dB half-power bandwidth of the frequency peak, and the dynamic flexural modulus is calculated from the resonant frequency.

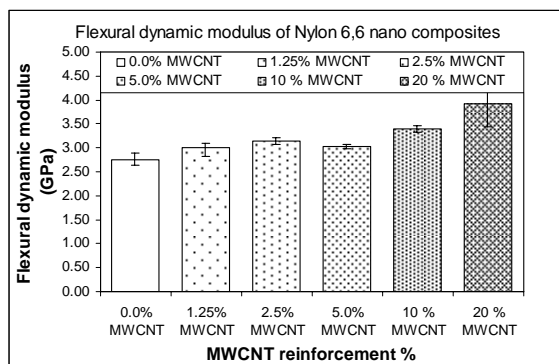


Fig. 1. Flexural dynamic modulus of nylon 6,6 nano composites.

The same (10"x1") flexural samples were also used for computing the dynamic extensional modulus and damping. In this setup, the sample was

tested in a free-free condition supported by nylon wires. Two extra masses were clamped at the ends of the sample for lowering the resonant frequencies within the range of interest. The accelerometer was placed at one end and an impact was given at the other end. In addition to the specimen dimensions the values of the two masses are also provided as input to the ICARUS program which has an algorithm taking into account the effect of end masses in computing the extensional modulus [2, 3]. Data was averaged for two tests with three specimens tested from each plate for both flexural and extensional data.

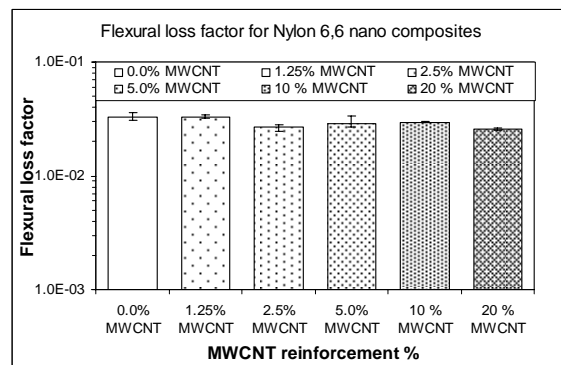


Fig. 2. Flexural loss factor of nylon 6,6 nano composites.

As shown in Figure 3, the extensional dynamic modulus of nylon 6,6 nano composites increased from 0 to 5% MWCNT loading. Further addition did not show any significant changes in extensional stiffness. On the other hand, extensional loss factor (Figure 4) showed a substantial drop for the 1.25% MWCNT, and then took an upward trend for higher loadings. It is not clear why this dramatic reduction in damping occurred for the 1.25% MWCNT samples.

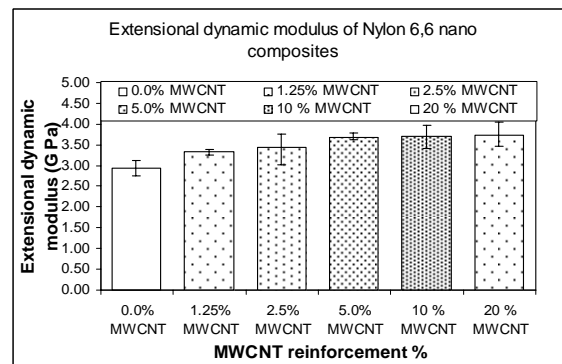


Fig. 3. Extensional dynamic modulus of nylon 6,6 nano composites.

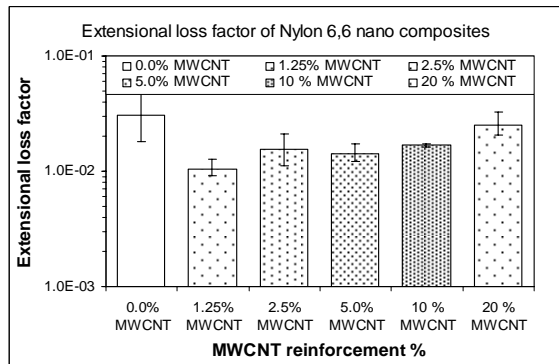


Fig. 4. Extensional loss factor of nylon 6,6 nano composites.

## 4 Low-velocity Impact and High-strain Rate Response

### 4.1 Low-velocity Impact

Specimens of dimensions 127 mm x 9.5 mm x 12.7 mm (5" x 3/8" x 0.5") for low-velocity impact testing were cut from the different nanoparticle enhanced plates and prepared in accordance to ASTM D-6110-06: Standard Test Method for Determining the Charpy Impact Resistance of Notched Specimens of Plastics. Both un-notched and notched samples were impacted. The notch, where applicable, was cut by specially made milling cutter with an angle of 45° and a depth of 2.54 mm (0.1") from top of plate, maintaining a 10.16 ± 0.05 mm (0.400" ± 0.002") thickness under the notch.

Low-velocity impact tests were performed in a Dynatup Model 8250 drop-weight impact system and the test method used was comparable to ASTM D6110-06 (the difference being that a drop-weight system was used here instead of a pendulum type machine recommended in the standard). In this test, the 127 mm (5") long specimens were impacted with a steel tup from a suitable drop height. After several trial runs, the cross-head weight and height were set such that about 6 Joules of impact energy was provided at a velocity of 2 m/s (4.5 mph). Five notched and un-notched samples were tested for each MWCNT weight loading.

Figures 5 and 6 show that the pure nylon 6,6 absorbed more load and energy to failure than MWCNT reinforced composites for both notched and un-notched specimens, with the 5 weight percent loading lower than the rest. Un-notched samples showed larger scatter and no significant conclusions can be drawn.

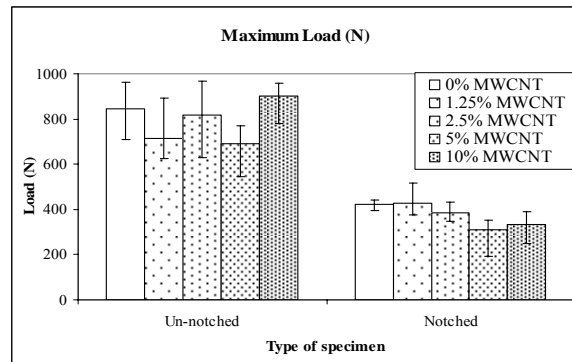


Fig. 5. Maximum loads for un-notched and notched nylon 6,6 nano composites under low-velocity (2 m/s) impact.

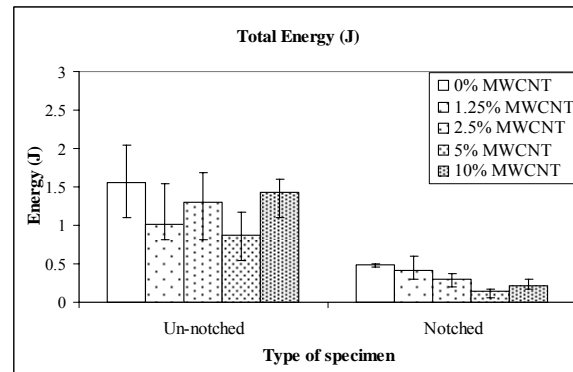


Fig. 6. Total absorbed energy for un-notched and notched nylon 6,6 nano composites under low-velocity (2 m/s) impact.

The fractured surfaces of un-notched samples were observed to be non-uniform while for the notched samples in most cases it was smooth. Analysis of fractured surfaces using atomic force microscopy is in progress to ascertain the role of MWCNT in the failure mechanism.

### 4.2 High-strain rate Compression Tests

The effect of varying weight percent of MWCNT on the strength, stiffness and energy absorption of nylon 6,6 was also analyzed at high-strain rates. Small size 127 mm x 12.7 mm (5" x 0.45" x 0.39") samples cut from the 0, 2.5, 5 and 10 weight percent nano composite plates were subjected to high-strain rate compression testing using the Split Hopkinson Pressure Bar apparatus [4]. It is to be noted that 1.25 weight percent nano samples were not available at time of high-strain rate testing, and therefore their data is not reported here. The strain rate for the tests was around 950/sec, with a minimum of 910 and maximum of 962, at a pressure setting of 30 psi.

Figure 7 shows a typical compressive strain vs time plot for the 10 weight percent MWCNT sample, and Figure 8 shows the associated stress-strain response. The addition of 2.5 weight percent MWCNT to pure Nylon 6,6 showed about 10-20% improvement in the strength and energy absorption at high-strain rates (Figures 9 and 10).

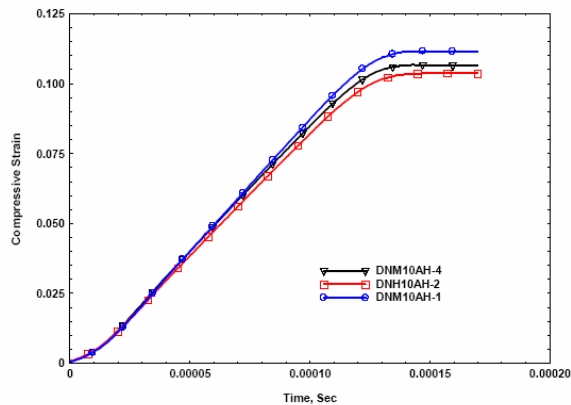


Fig. 7. Compressive strain vs time response of the 10 weight percent nylon 6,6 nano composite at high-strain rate (~ 950/sec) from the Hopkinson pressure bar tests.

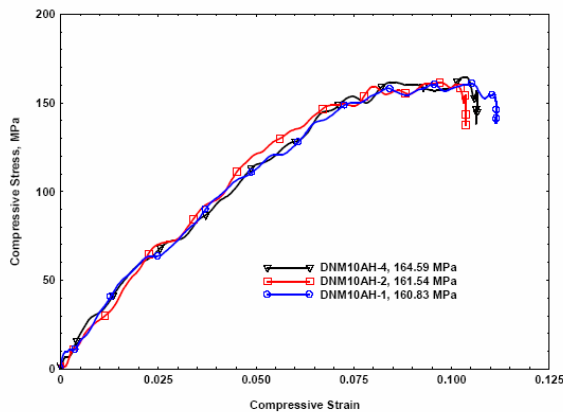


Fig. 8. Compressive stress-strain response of the 10 weight percent nylon 6,6 nano composites at high-strain rate (~ 950/sec) from the Hopkinson pressure bar tests.

Higher weight percents of MWCNT did not proportionately improve the strength or energy absorption. It is interesting to note that the dynamic compressive modulus (Figure 11) for 5 weight percent nano composite is about the same as pristine nylon 6,6 at these high-strain rates. All nano samples, including nylon 6,6, exhibited permanent-set deformation under the Hopkinson bar high-strain rate compressive loading with none of them shattering during testing.

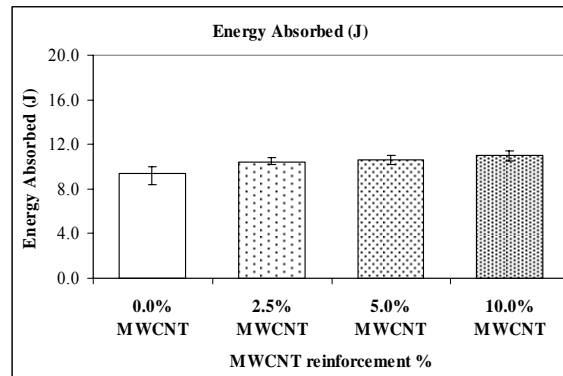


Fig. 9. Energy absorbed by nylon 6,6 nano composites at high-strain rate (~ 950/sec) from the Hopkinson pressure bar tests.

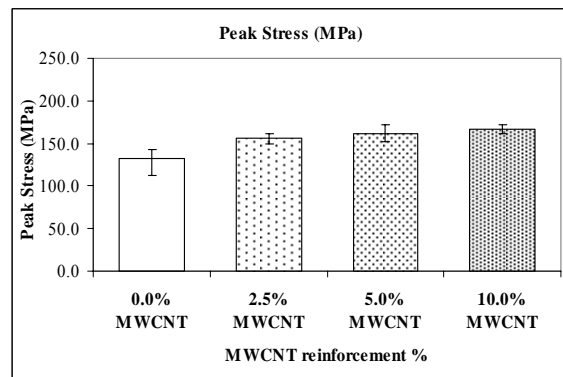


Fig. 10. Peak stress of nylon 6,6 nano composites at high-strain rate (~ 950/sec) from the Hopkinson pressure bar tests.

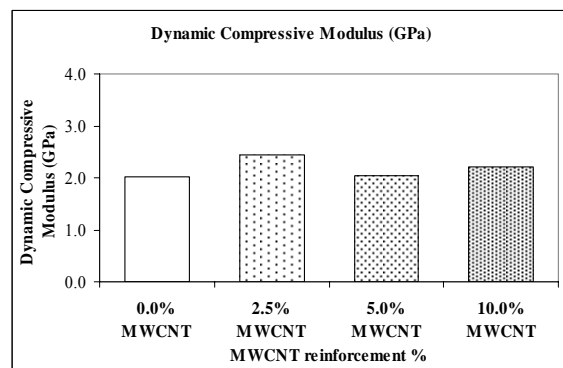


Fig. 11. Dynamic compressive modulus of nylon 6,6 nano composites at high-strain rate (~ 950/sec) from the Hopkinson pressure bar tests.

## 5 Molecular Simulations of Nano Composites

The commercially available Material Studio Software® [5] has been used for performing molecular dynamic simulations of single- and multi-wall carbon nanotube reinforced polymers to predict their mechanical properties. This was accomplished by using bulk amorphous polymer structures generated by constructing polymeric chains in a periodic cell, taking in to account the bond torsion probabilities and bulk packing requirements. Models are then equilibrated by a series of energy minimization and molecular dynamic runs. Crystal structures for semi-crystalline and amorphous polymers are generated [6-11] and the simulated bulk structures subjected to three different methods for evaluating their mechanical behavior: the static method; the fluctuation method; and the dynamic method.

After molecular dynamics simulation has been performed, the resulting deformed molecular structure is analyzed for determining elastic constants. Elastic constants of the final atomic configuration are computed using the static approach suggested by Theodorou and Suter [12]. The elastic constants in this approach are defined as:

$$C_{lmnk} = \left. \frac{\partial \sigma_{lm}}{\partial \varepsilon_{nk}} \right|_{T, \varepsilon_{nk}} = \frac{1}{V_o} \left. \frac{\partial^2 A}{\partial \varepsilon_{lm} \partial \varepsilon_{nk}} \right|_{T, \varepsilon_{lm}, \varepsilon_{nk}} \quad (1)$$

where,  $A$  denotes the Helmholtz free energy,  $\varepsilon$  is the strain component,  $\sigma$  is the stress component and  $V_o$  is the volume of the simulation cell in the undeformed configuration. It is assumed that contributions originating from changes in configurational entropy on deformation, and from the strain dependence of the vibrational frequencies are negligible for glassy polymers. Thus, it is possible to estimate the elastic stiffness coefficients from numerical estimates as:

$$\frac{d^2 U}{d \varepsilon_i d \varepsilon_j} = \frac{d \sigma_i}{d \varepsilon_j} \quad (2)$$

where,  $U$  is the potential energy of the system.

For each configuration submitted for analysis of static elastic constants, the first step consists of energy minimization using conjugate gradients method. In this study, the target minimum derivative for the initial step is 0.1 kcal/Å. However, to reduce the time required for the calculation, a maximum of 1000 steps were performed in attempting to satisfy

the convergence criterion. Following the initial stage, three tensile and three pure shear deformations of magnitude  $\pm 0.0005$  were applied to the minimized system and the system was re-minimized following each deformation. The internal stress tensor was then obtained from the analytically calculated virial and used to obtain estimates of the 6 x 6 elastic stiffness coefficient matrices.

As a result of these simulations, the elastic stiffness coefficients could be obtained by estimating the second derivatives of the deformation energy with respect to strain using a finite difference formula (for diagonal components only), and by calculating  $\Delta \sigma_i / \Delta \varepsilon_j$  for each of the applied strains, where  $\sigma_i$  represents, in vector notation, elements of the stress tensor obtained analytically using the following expression:

$$\sigma = -\frac{1}{V_o} \left[ \left( \sum_{i=1}^N m_i (v_i v_i^T) \right) + \left( \sum_{i < j} r_{ij} f_{ij}^T \right) \right] \quad (3)$$

where, index  $i$  runs over all particles 1 through  $N$ ;  $m_i$ ,  $v_i$  and  $f_i$  denote the mass, velocity and force acting on particle  $i$ ; and  $V_o$  denotes the (undeformed) system volume. In an atomistic calculation, this expression for internal stress tensor is called virial expression.

Generally, it is assumed that the numerical estimation of second derivatives (of the energy) will be less precise than estimation of the first derivatives (of the stress). Therefore, the latter method has been used here for calculating the elastic constants. This approach creates the foundation of calculating elastic constants; however, the potential energy expression can alter depending upon the ensemble of thermodynamic variables of the simulation experiment.

Various trial runs were carried out for the simulation of multi-wall carbon nanotubes. Finally, a MWCNT with 3 walls was simulated and the elastic constants were calculated. Two types of simulations are used: a sequential simulation in which the number of walls and Chirality of inner tube are specified, then the program automatically calculates inter-layer distances and chirality of subsequent layers; in the second approach the three walls of the MWCNT are assigned as 5-5, 10-10 and 15-15, respectively (Figure 12). The number of walls is limited to 3 because placing any larger size MWCNT in the polymer would generate a computationally intensive system. For the case



shown in Figure 12, 2400 atoms were simulated in a  $22.7 \text{ \AA} \times 22.7 \text{ \AA} \times 50.2 \text{ \AA}$  unit cell.

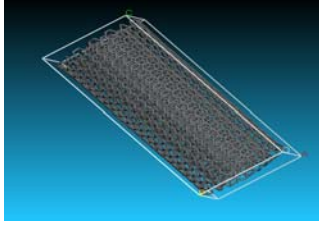


Fig. 12. MD simulation of MWCNT

Stiffness matrices for assigned and sequential simulations are shown below for a MWCNT aligned in a Cartesian coordinate system with the 1 axis along the length of the nano tube.

*Assigned simulation:*

$$C_{ij} = \begin{bmatrix} 537 & 42 & 60 & -3 & -2 & 3 \\ 113 & 175 & 207 & 13 & 11 & 12 \\ -2 & 185 & 132 & -12 & -6 & 17 \\ -10 & 4 & 8 & -9 & 16 & -8 \\ 58 & -7 & 55 & 2 & 82 & 13 \\ 13 & 20 & 7 & 2 & 16 & -6 \end{bmatrix} \text{ GPa}$$

*Sequential simulation:*

$$C_{ij} = \begin{bmatrix} 226 & 4 & 3 & 1 & 1 & -1 \\ 4 & 35 & 30 & 0 & 1 & 0 \\ 4 & 30 & 35 & 1 & 1 & -1 \\ 1 & 0 & 0 & 0 & -1 & 0 \\ 0 & 1 & 1 & -1 & 0 & 0 \\ 0 & 0 & 0 & 0 & 0 & 1 \end{bmatrix} \text{ GPa}$$

Comparing the two approaches, it is observed that there is a big difference between them. The sequential simulation appears to give values that are more realistic. The only significant values are those occupying the  $3 \times 3$  left-upper corner sub-matrix, from which it can be concluded that MWCNT is transversely isotropic as expected.

The elastic constants of nylon-6,6 thermoplastic and styrenated vinyl ester thermo-set with varying weight percents of single- and multi-wall carbon nano tubes are under investigation. For the nylon-6,6, a single chain of twenty monomers is built (Figure 13-a), and minimized using the conjugate gradient method.

A rectangular unit cell of dimensions  $33.3 \text{ \AA} \times 33.3 \text{ \AA} \times 33.3 \text{ \AA}$  was constructed from 10 polymer chains with 3820 atoms and initial density of  $1.2 \text{ gm/cc}$  (Figure 13-b). The unit cell was minimized for 150 pico-seconds at a rate of 1 femto-second under NPT (constant Number of particles, constant Pressure and constant Temperature) conditions using Condensed-phase Optimized Molecular Potentials for Atomistic Simulation Studies (COMPASS) force field [13]. Then, dynamic temperature loading was applied on the unit cell as follows: First, the temperature was increased from room temperature to  $80 \text{ C}$ , which is beyond the glass transition temperature of nylon-6,6. This was done in two steps at a rate of 150 pico-seconds per step, then cooled to room temperature at the same rate.

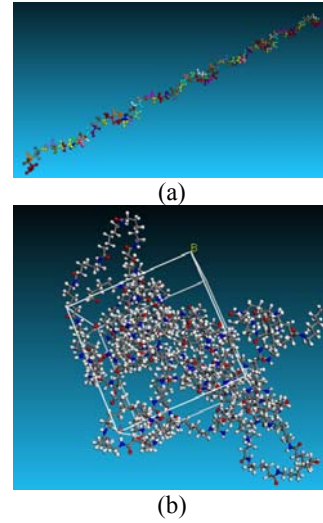


Fig. 13. MD simulation of (a) single, and (b) ten chains of nylon-6,6 polymer.

The van der Waals interaction potential is relatively short range and dies out at a separation distance of  $8\text{-}10 \text{ \AA}$ . Choosing how to treat long-range nonbond interactions is an important factor in determining the accuracy of energy evaluation. The obtained stiffness matrix of nylon-6,6 is shown below:

$$C_{ij} = \begin{bmatrix} 3.38 & 1.83 & 2.19 & 0.28 & 0.26 & 0.48 \\ 1.92 & 3.83 & 1.79 & 0 & 0 & 0.67 \\ 2.32 & 1.97 & 3.57 & 0.10 & 0 & 0.07 \\ 0.24 & 0 & 0.06 & 1.09 & 0.2 & 0 \\ 0.27 & 0.08 & 0.08 & 0.22 & 1.12 & 0.06 \\ 0.49 & 0.66 & 0.02 & 0 & 0.06 & 1.2 \end{bmatrix}$$

A box-shaped unit cell was used to embed a single MWCNT in nylon 6,6 matrix. The three edges (a, b and c) of the cell were aligned respectively with the three coordinate axes (x, y and z), with the nanotube axis aligned along the z cell edge length (Figure 14). The MWCNT is generated sequentially with the inner diameter having Chirality 5-5. Concentration of nylon 6,6 was then changed to match the desired weight fraction of nano composites. Periodic boundary conditions were applied across all faces of the cell. Different weight fractions of reinforcements: 1.25, 2.5, 5 and 10% are being modeled.

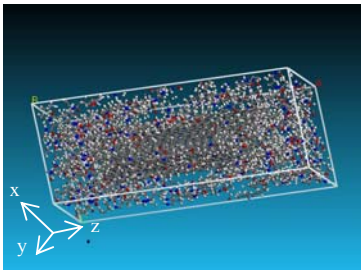


Fig. 14. MD simulation of nylon 6,6 reinforced with MWCNT.

The atomic configuration within the cell, corresponding to the cross-linked molecules of nylon matrix and MWCNT, was generated using the following procedure:

- a. A single molecule of the nylon is first constructed using the Visualizer [5] program from Accelrys, Figure 13-a;
- b. Next, the molecule generated in (a) is duplicated several times depending on the weight fraction of interest, Figure 13-b;
- c. The nylon-6,6 molecules generated in (b) are used as fragments within the Amorphous Cell [5] program from Accelrys to generate a box-shape computational cell of a given size containing the nylon 6,6 of a specified density;
- d. Atomic configuration corresponding to the MWCNT is then constructed using the procedure described earlier;
- e. Segments of the molecules generated in (c) are next translated and rotated in order to create a "hole" in the center of the cell into which the MWCNT atomic configuration generated in (d) is inserted; and
- f. The atomic configuration obtained in (e) is subjected to a series of energy minimization

and dynamic relaxations under NPT condition starting with 20 pico second for 1 femto second time step. The temperature was raised from room temperature to 80 C (beyond the glass transition temperature of nylon 6,6), then cooled down to room temperature.

All the molecular simulations are carried out using the Discover program by Accelrys [5]. The potential energy minimization within Discover is carried out by combining the Steepest Descent, Conjugate Gradient and the Newton's minimization algorithms. These algorithms are automatically inactivated/ activated as the atomic configuration is approaching its energy minimum (i.e. the Steepest Descent method is activated at the beginning of the energy minimization while the Newton's method is utilized in the later stages of the simulation). Simulations of nylon 6,6 with different weight percents of MWCNT are in progress and results will be presented at the conference.

## 6 Conclusions

Non-destructive vibration response results show that the dynamic stiffness of nylon 6,6 nano composites increases with MWCNT loadings and the damping is reduced. In general, the 10 and 20 weight percent MWCNT/nylon 6,6 composites exhibited highest stiffness and damping. The 20 weight percent nano composite plates had broken into pieces during extrusion manufacturing process, and are therefore not considered practical.

Addition of MWCNT was detrimental to the maximum load and energy absorption under low-velocity impact. However, there was an improvement in the strength and energy absorption at high-strain rates under compressive loading with the Hopkinson pressure bar apparatus.

Results obtained from various types of loadings applied to MWCNT show that they are transversely isotropic. The transverse properties of MWCNT are comparatively poor.

## 7 Acknowledgement

Authors wish to acknowledge support for this research by ONR Grant# N00014-06-1-0577, Office of Naval Research, Solid Mechanics Program (Dr. Yapa D.S. Rajapakse, Program Manager). Ravi Zalani, Swasti Gupta and Hunain Alkhateb are the graduate students who worked on this project. The persistent effort by Dr. Larry Drzal's group at Michigan State University for manufacturing nanoparticle enhanced vinyl ester composite plates is appreciated. Hopkinson bar high-strain rate testing was performed by Dr. David Hui's group at University of New Orleans.

## References

- [1] Mantena P. R., Mann R. and Nori C. "Low-velocity impact response and dynamic characteristics of glass resin composites". *Journal of Reinforced Plastics and Composites*, Vol. 20, No. 6, pp. 513-534, 2001.
- [2] Nori C., Mantena P. R. and McCarty T. A. "Experimental and finite element analysis of pultruded glass-graphite/epoxy hybrids in axial and flexural modes of vibration". *Journal of Composite Materials*, Vol. 30, No. 18, pp. 1996-2018, 1996
- [3] Suarez S. A. and Gibson R.F. "Improved impulse-frequency response techniques for measurement of dynamic mechanical properties of composite materials". *Journal of Testing and Evaluation*, Vol. 15, pp. 114-121, 1987
- [4] Dutta P.K. and Hui D. "Stress wave propagation through the thickness of graphite/epoxy laminated plates using PVDF sensors" *Proceedings of the Sixth Japan-US Conference on Composite Materials*, June 22-24, Orlando, FL, Technomic Publishing, pp. 845-854, 1992.
- [5] MS Modeling 4.0 Online Help Manual, Accelrys Inc., 2005
- [6] Pal G., Al-Ostaz A., Mantena P.R., Cheng A. and Song C. "Molecular dynamic simulations of SWCNT-polymer nanocomposite and its constituents". *Proceedings of the 21<sup>st</sup> Annual Technical Conference of the American Society for Composites, Dearborn, MI*, Paper #136 on CD ROM, 2006.
- [7] Rappe, A. K., Casewit C. J., Colwell K.S., Goddard W.A. and Skiff W.M. "UFF - a full periodic table force field for molecular mechanics and molecular dynamics simulations". *Journal of the American Chemical Society*, 114: 10024 - 10035, 1992
- [8] Anderson H. C. "Molecular dynamics simulations at constant pressure and/or temperature". *Journal of Chemical Physics*, 72(4): 2384-2393, 1980
- [9] Parrinello M. and Rahman A. "Strain fluctuations and elastic constants". *Journal of Chemical Physics*, 76(5): 2662 - 2665, 1982.
- [10] Gou, J., Jiang S., Minaie B., Liang Z., Chuck Z. and Wang B. "Nano-scale modeling and simulation interfacial bonding of single walled nanotube reinforced composites". *Proceedings of IMECE2003 International Mechanical Engineering Congress and Exposition*, Washington, D.C., IMECE'03-41138, pp 1 -5, 2003.
- [11] Liao K. and Li S. "Interfacial characteristics of a carbon nano-tube polystyrene composite system". *Applied Physics Letters*, 79(25): 4225 - 4227, 2001.
- [12] Theodorou, D. N., and Suter U.W. "Atomistic Modeling of Mechanical Properties of Polymeric Glasses". *Macromolecules*, 19: 139 - 154, 1986.
- [13] Sun H. "COMPASS: An *ab initio* force-field optimized for condensed-phase applications - Overview with details on alkaline and benzene compounds," *Journal of Physical Chemistry B*, 102: 7338 - 7364, 1998